Struct Multidisc Optim (2009) 38:347–356
DOI 10.1007/s00158-008-0279-7

RESEARCH PAPER

Systematic design of distributed piezoelectric modal sensors/actuators for rectangular plates by optimizing the polarization profile

A. Donoso · J. C. Bellido

Received: 5 February 2008 / Revised: 8 April 2008 / Accepted: 26 April 2008 / Published online: 21 June 2008

Abstract In this paper the problem of finding the shape of distributed piezoelectric modal sensors/actuators for plates with arbitrary boundary conditions is treated by an optimization approach. A binary function is used to model the design variable: the polarization profile of the piezoelectric layers. Contrary to what it could be expected, it is analytically proved that it is possible to find manufacturable polarization profiles taking on only two values, i.e. either positive or negative polarization. Several numerical examples are shown to corroborate that such topologies isolate particular vibration modes in the frequency domain.

Keywords Piezoelectricity · Modal sensors/actuators · Relaxed formulation · Polarization profile

1 Introduction

Piezoelectricity is the ability of some materials (notably crystals and certain ceramics) to generate an electric potential in response to applied mechanical stress and vice versa. Whenever this kind of materials produce an electric signal proportional to their deformation, it is said that they work as sensors, and conversely, when they convert electrical energy into mechanical one, as actuators. An interesting application is the vibration control in structures (Moheimani and Fleming 2006). This way to do control, called active control (or active damping), consists of adding piezoelectric sensors and actuators to the structure to be controlled. The sensors and actuators may consist of a number of discrete transducers or a distributed transducer material. In the first case, both the location and the gain have to be determined for each discrete transducer (Friswell 2001; Gawronski 2000). On the contrary, to understand how a distributed transducer works (Lee and Moon 1990), let us consider a plate-type structure with two piezoelectric layers bonded to both top and bottom surfaces, respectively. When an electric field is applied to the piezoelectric lamina that is working as actuator, only the part of the lamina that is covered by electrode will be affected by the electric field, and consequently, only that region will undergo mechanical stresses. A similar effect can be found in the piezoelectric sensor. Rather than discrete transducers, distributed transducers are designed by shaping the surface electrode (sometimes also the polarization profile) of the piezoelectric layers, which let us determine both location and gain at the same time, reducing in that way the signal processing requirements.

In active control, it is desirable to avoid the problem of spill over, that is, filter high-frequency unmodeled modes which affect the stability of the closed-loop system. One way to do that is by using the so-called modal sensors/actuators (Lee and Moon 1990) (hereafter MSA). More applications can be found in Clark et al. (1998).

A. Donoso (✉) · J. C. Bellido
Departamento de Matemáticas, ETS de Ingenieros Industriales, Universidad de Castilla La Mancha, 13071 Ciudad Real, Spain
e-mail: Alberto.Donoso@uclm.es

J. C. Bellido
e-mail: JoseCarlos.Bellido@uclm.es

MSA are those which measure/excite a single mode of a structure and also avoid the problem of spill over. It is worth to note that a reciprocal relationship exits between a modal sensor and a modal actuator, that is to say, the sensor shape that observes a particular mode (modal sensor) is the same as the actuator shape that excites that particular mode (modal actuator), so in terms of the design we just have to focus on one of them.

To design a modal sensor (for instance) two main variables, among others, must be taken into account: the effective surface electrode that is modeled by a binary function $F(x, y)$ (F equals 1 if (x, y) is covered by electrode, otherwise it is 0), and the polarization profile of the piezoelectric layers, modeled by another binary function $P_0(x, y)$ (which typically takes on the values -1 and 1 only).

For beams and one-dimensional plates (basically treated as beams with a slight modification in the flexural rigidity term), the problem of finding MSA reduces to computing the normalized surface electrode width, $\mathcal{F}(x)$ (which is given by the integral of $F(x, y)P_0(x, y)$ along the y-direction), with x being the longitudinal axis of the structure. For such cases, it is proved both theoretically and experimentally in Lee and Moon (1990) that either the modal actuator profile or the modal sensor profile is found as a constant times the second derivative of that particular mode shape (or the curvature). Now the function $\mathcal{F}(x)$ contains all the necessary information to construct MSA: on the one hand, its absolute value indicates the gain distribution of the transducer and on the other hand, it forces the polarization profile (positive or negative) of the piezoelectric layers to vary along the x-direction in accordance with its profile. As an illustrative example, the two first MSA for a one-dimensional cantilever plate are shown in Fig. 1a. We can see that for isolating the first mode, both region 1 and region 2 have to be activated with the same polarity, whereas for the second mode, we have to activate both region 1 and region 3 with opposite polarity. Tip-response in the frequency domain is plotted in Fig. 1b, corroborating what we have expected.

Basically, the condition which lets us construct MSA is the orthogonality principle among the vibration mode shapes of the structure to be controlled. This orthogonality principle can be easily proved for beams (and one-dimensional plates) whichever the boundary conditions we consider, as well as for plates with pinned boundary conditions, because in such cases the modes are given by sinosoid functions, and of course, they verify the criterion. However, a general orthogonality principle does not exist for the vibration mode shapes

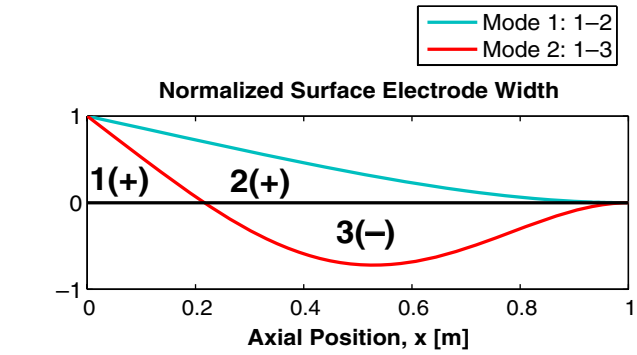

(a)

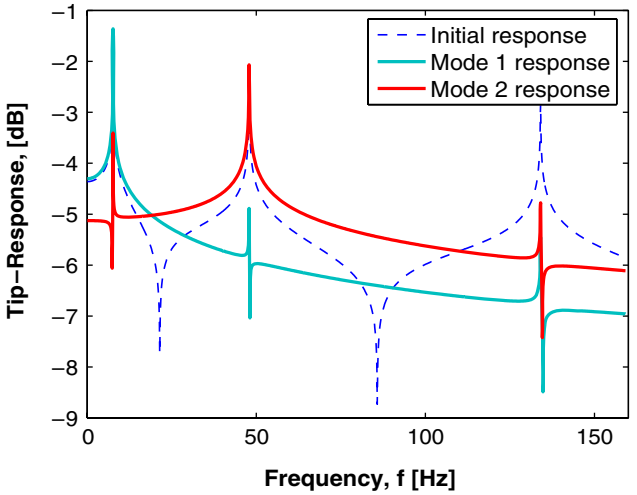

(b)

Fig. 1 The first two MSA for a one-dimensional cantilever plate. **a** Electrode shape. **b** Frequency response

of plates (Blevins 1985; Clark and Burke 1996), because of the complexity of the boundary conditions, and therefore, we can not state that

$$\int_S \phi_{rj}\,\phi_{mn}\,dx\,dy = 0, \quad \text{for} \quad r \neq m,\ j \neq n, \tag{1}$$

is true in general, where ϕ_{rj} is the mode shape of the rj mode and S is the area covered by the piezoelectric layers.

Many authors have studied the problem of designing MSA for two-dimensional structures (see Jian and Friswell 2007 as an excellent and recent survey of it), but to date, it has not been found a systematic way to do it. In the pioneering work (Lee and Moon 1990) it is suggested a way to create ideal MSA for a four-sided simply-supported rectangular plate. As commented above, the particular boundary conditions for this situation make it possible to obtain theoretically a family of MSA. The problem now is that normalized MSA take values in a continuous interval, for instance, between -1 and 1, that is, $FP_0(x, y) \in [-1, 1]$. One

possible physical interpretation is to assume $F \equiv 1$ and to require a precisely-implemented variation in the polarization profile, P_0, over x and y, but as pointed out in Clark and Burke (1996), that could be really difficult to achieve in practice, from a manufacturing point of view.

To overcome this problem, two design methods are proposed in Kim et al. (2001). The first one optimizes electrode surface, poling direction as well as lamination angle of piezoelectric multi-layers, and the second one optimizes the gain weight on each segment electrode in which a piezoelectric single-layer is divided. Even though the results obtained are satisfactory, the way to implement the topologies obtained requires extra interface circuits and complicates electrode patterns as using genetic algorithms over rough meshes.

An interesting alternative is explored in Sun et al. (2002), where a piezoelectric layer of variable thickness is proposed to design MSA, but again, since such a layer would be very difficult to implement in practice, it is replaced by another layer made up with many small patches of different and uniform thickness. Other possibilities are suggested in Preumont et al. (2003), where a new porous distributed electrode concept is introduced, which allows the effective piezoelectric coefficient to be tailored, and in Hsu and Lee (2004), where a new distributed sensor is introduced by superposition of even and odd strain functions. In line with distributed transducers, some authors have begun to apply topology optimization to find optimal piezo-actuator distributions in plates and shells for the static case (Kögl and Silva 2005), and, more recently, in beams for both static and dynamic loads (Donoso and Sigmund 2008). In Mukherjee and Joshi (2003) shape optimization techniques are also used to optimize the shape of piezoelectric actuators over beams and plates in order to achieve desired shapes of the structure.

Looking back to the design of MSA, an obvious but natural optimization approach is proposed in the recent references Jian and Friswell (2006) and Jian and Friswell (2007). In those works, the continuous shape of a sensor is optimized, being a limited number of points of the parameterized boundary the design variables. Although the polarization profile is also initially considered in the model, it is not used in the optimization process as a design variable.

Following the models considered in Jian and Friswell (2006) and Kim et al. (2001), and using the philosophy of the topology optimization problems (the reader is referred to Bendsøe and Sigmund (2003) for an excellent overview of the method and different applications), the aim of this paper is to propose a systematic way to design MSA through an appropriate optimization approach that decides which regions of the piezoelectric layers have to be covered by electrode and which ones not, and in the former case, which parts of the transducer material must be polarized in upward direction, and which ones in opposite direction. The paper is organized as follows: in the next section an optimization approach is proposed and the physics of the problem is briefly discussed. Later on, a relaxed formulation for the optimization problem is presented, letting us analytically prove that the original optimization approach admits solutions in terms of the binary functions taken as design variables. Finally, several numerical examples for a plate with different boundary conditions are included to illustrate that the topologies obtained make it possible to isolate particular modes in the frequency domain.

2 Modeling the design of MSA as an optimization problem

We consider a thin rectangular plate with two piezoelectric layers bonded to both top and bottom surfaces as shown in Fig. 2. Focusing on the sensor layer, such a distributed transducer collects the charge by an effective surface electrode, performing the signal processing through the integration in the spatial domain (not in time), so that the response of the piezoelectric sensor can be expressed as (Lee and Moon 1990)

$$q(t) = -\frac{(h_p + h_s)}{2} \times \int_0^{L_x}\int_0^{L_y} F P_0(x,y)\left(e_{31}\frac{\partial^2 w}{\partial x^2} + e_{32}\frac{\partial^2 w}{\partial y^2} + 2e_{36}\frac{\partial^2 w}{\partial x \partial y}\right) dy\, dx, \quad (2)$$

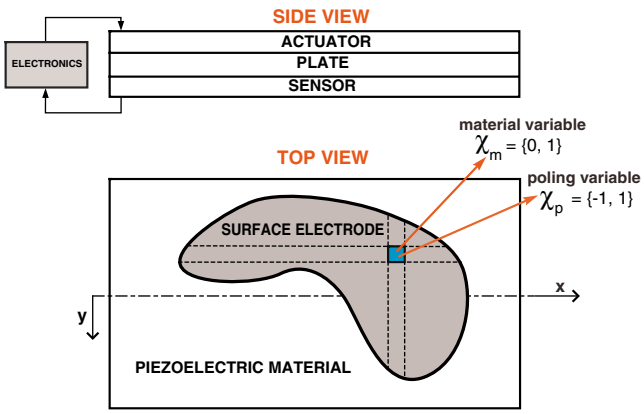

Fig. 2 Design domain

where q is the sensor output charge, h_p is the thickness of the plate, h_s is the thickness of the sensor, w is the out-of-plane displacement of the plate, L_x and L_y are the lengths of both sides of the plate, and e_{31}, e_{32} and e_{36} are the piezoelectric stress/charge constants. In the following, we will assume that $e_{31} = e_{32} = e$ (i.e. the piezo's charge per unit area is the same in both directions) and $e_{36} = 0$ (i.e. the sensor's piezoelectric axes are coincident with the geometric axes of the plate). We will also consider that the piezoelectric layers have negligible stiffness and mass compared to the ones of the plate.

The out-of-plane displacement of the plate, w, can be written by a modal expansion

$$w(x, y, t) = \sum_{j=1}^{\infty} \phi_j(x, y)\ \eta_j(t), \tag{3}$$

where $\phi_j(x, y)$ and $\eta_j(t)$ are the j-th mode shape and the j-th modal coordinate, respectively. Inserting (3) in (2), we have

$$\begin{aligned} q(t) = &-e\frac{(h_p + h_s)}{2} \\ &\times \int_0^{L_x}\int_0^{L_y} FP_0(x, y) \sum_{j=1}^{\infty} \left(\frac{\partial^2 \phi_j}{\partial x^2}\eta_j(t) + \frac{\partial^2 \phi_j}{\partial y^2}\eta_j(t) \right) \\ &\times dy\ dx = -e\frac{(h_p + h_s)}{2} \\ &\times \sum_{j=1}^{\infty} \left\{ \int_0^{L_x}\int_0^{L_y} FP_0(x, y) \left(\frac{\partial^2 \phi_j}{\partial x^2} + \frac{\partial^2 \phi_j}{\partial y^2} \right) \right. \\ &\left. \times\ dy\ dx \right\} \eta_j(t), \end{aligned} \tag{4}$$

arriving at

$$q(t) = -e\frac{(h_p + h_s)}{2} \sum_{j=1}^{\infty} B_j\ \eta_j(t), \tag{5}$$

with

$$B_j = \int_0^{L_x}\int_0^{L_y} \chi_m(x, y)\ \chi_p(x, y)\ \triangle\phi_j(x, y)\ dy\ dx, \tag{6}$$

where F and P_0 have been renamed by the binary functions χ_m and χ_p, respectively (see Fig. 2), such that $\chi_m(x, y) \in \{0, 1\}$ (to put or not electrode) and $\chi_p(x, y) \in \{-1, 1\}$ (positive or negative polarization). Truncating (5) in the first M modes, the following optimization approach

$$\text{Maximize}_{\chi_m,\ \chi_p} \quad B_k(\chi_m, \chi_p) \tag{7}$$

subject to:

$$B_j(\chi_m, \chi_p) = 0, \quad \text{for } j = 1, \cdots, M, \text{ and } j \neq k, \tag{8}$$

is proposed to find an ideal modal sensor that observes the k-th mode (i.e. the coefficient B_k is maximized) among the first M modes and filters the rest of them (i.e. the rest of coefficients B_j with $j \neq k$ are canceled). Likewise, such profiles (defined through their corresponding patterns χ_m and χ_p) let the actuator layer of thickness h_a control both the magnitude and the location of the forces induced by the electric field $\mathcal{E}(t)$ to the plate through the actuator equation (Lee and Moon 1990)

$$\begin{aligned} &\frac{Eh_p^3}{12(1-\nu^2)} \left(\frac{\partial^4 w}{\partial x^4} + 2\frac{\partial^4 w}{\partial x^2 \partial y^2} + \frac{\partial^4 w}{\partial y^4} \right) + \rho h_p \frac{\partial^2 w}{\partial t^2} \\ &\quad = -h_p h_a (h_p + h_a) e \mathcal{E}(t)\ \triangle(\chi_m \chi_p(x, y)), \end{aligned} \tag{9}$$

and therefore, to excite the mode at interest.

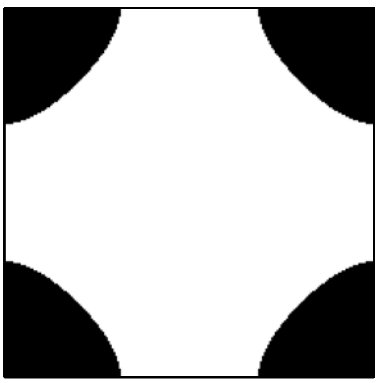

(a) $M = 10$

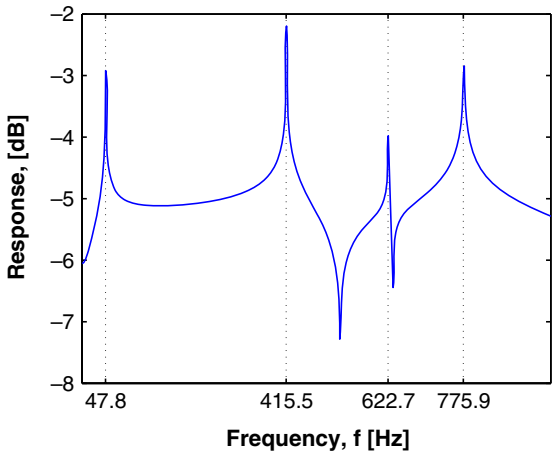

(b) $M = 10$

Fig. 3 Polarization profiles to isolate the first mode for a four-side simply-supported plate when considering $M = 10$ (**a**, **b**)

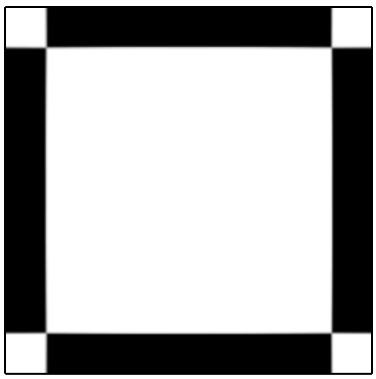

(a) $M = 15$

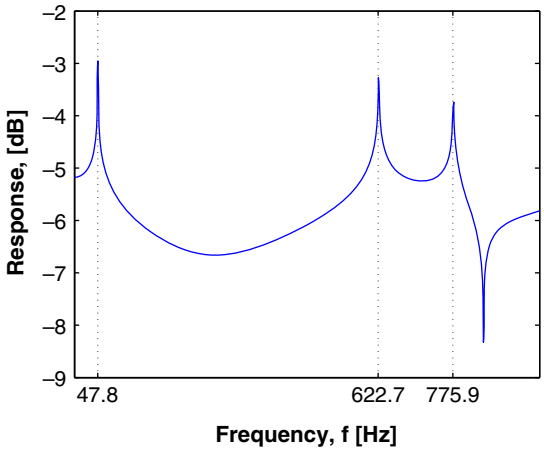

(b) $M = 15$

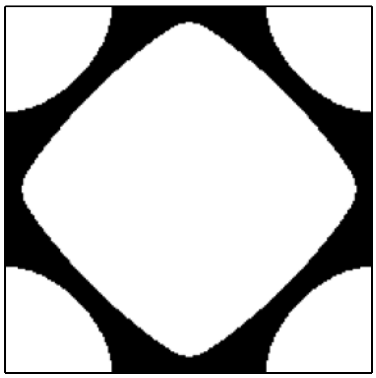

(c) $M = 20$

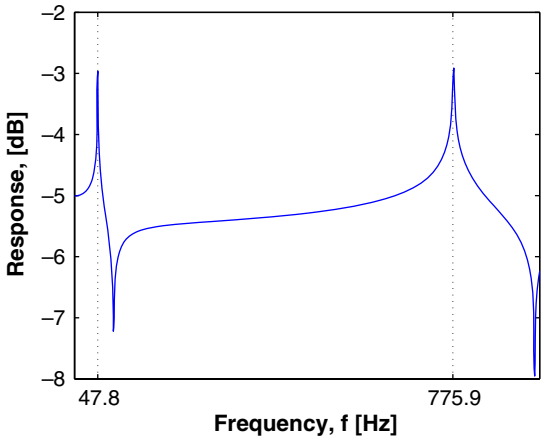

(d) $M = 20$

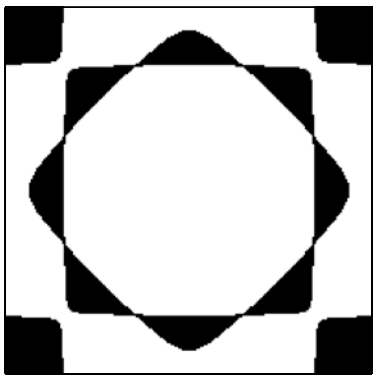

(e) $M = 26$

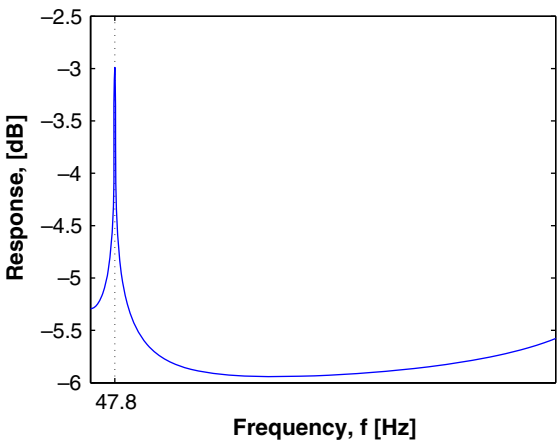

(f) $M = 26$

Fig. 4 Polarization profiles to isolate the first mode for a four-side simply-supported plate when considering $M = 15$ (**a**, **b**), $M = 20$ (**c**, **d**) and $M = 26$ (**e**, **f**)

3 Mathematical analysis of the optimization problem

In order to analyze from a mathematical point of view our optimization problem (7), it is convenient to put variables χ_m and χ_p together into a single one, $\chi(x, y) = \chi_m(x, y)\ \chi_p(x, y)$. This makes perfect sense as both variables appear together as a product both in the functional B_k and in the constraints. Now variable χ may take on any of the three values $-1, 0, 1$, with

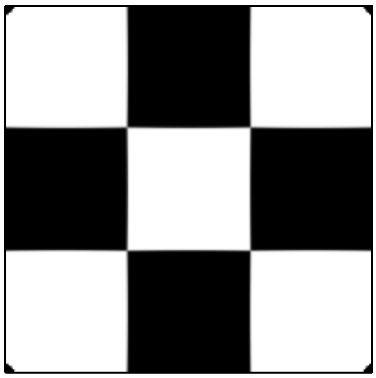

(a) $M = 26$

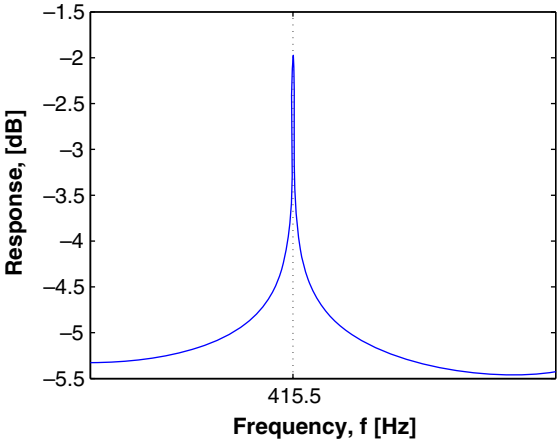

(b) $M = 26$

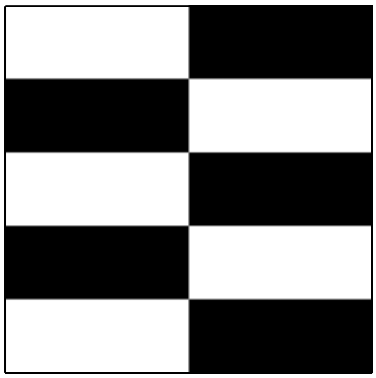

(c) $M = 26$

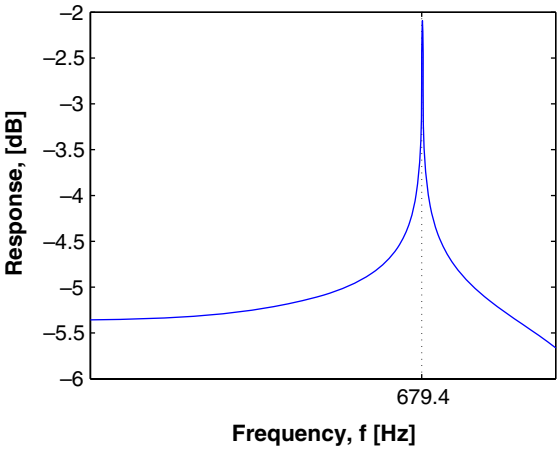

(d) $M = 26$

Fig. 5 Polarization profiles to isolate the eleventh mode (**a**, **b**) and the eighteenth mode (**c**, **d**) for a four-side simply-supported plate

obvious meaning for any of those values. The optimization problem (7) is then rewritten as

$$\text{Maximize}_{\chi\in\{-1,0,1\}} \quad B_k(\chi)$$

subject to:

$$B_j(\chi) = 0, \quad \text{for } j = 1, \cdots, M, \text{ and } j \neq k. \tag{10}$$

We cannot guarantee, in principle, the existence of optimal solutions for optimization problem (7) since the set of functions where we optimize,

$$\mathcal{U} = \left\{\chi \in L^\infty((0, L_x) \times (0, L_y)) \ : \ \chi(x, y) \in \{-1, 0, 1\}\right\}$$

is not compact in the weak-$\star$ topology of $L^\infty((0, L_x) \times (0, L_y))$ (the space of measurable and bounded functions defined on $(0, L_x) \times (0, L_y)$). Therefore, in order to have a well-posed optimization problem, we need to find a relaxed formulation of problem (7), what in this case is pretty simple and it consists of enlarging the set where we minimize to its closure in the weak-$\star$ topology of L^∞, i.e. to

$$\overline{\mathcal{U}} = \left\{\rho \in L^\infty((0, L_x) \times (0, L_y)) \ : \ -1 \leq \rho(x, y) \leq 1\right\}.$$

Then the relaxed formulation of problem (7) is

$$\text{Maximize}_{\rho\in\overline{\mathcal{U}}} \quad B_k(\rho) \tag{11}$$

subject to:

$$B_j(\rho) = 0, \quad \text{for } j = 1, \cdots, M, \text{ and } j \neq k. \tag{12}$$

In this problem we have just replaced the set where we optimize in problem (7), $\mathcal{U}$, by the larger set $\overline{\mathcal{U}}$. (see Fonseca and Leonni 2007; Tartar 2000). As we have mentioned above, problem (11) is a relaxation of (7), meaning that:

1. problem (11) admits optimal solutions;
2. the maximum value for (11) equals to the supremum value for (7);

3. any maximizer for problem (11) is the (weak-$\star$) limit of a maximizing sequence for (7) and vice-versa, any maximizing sequence for (7) converges to a maximizer for (11).

Problem (11) consists of maximizing a linear function on the set $\overline{\mathcal{U}}$ under linear constraints, and in such a simple situation we can state the following result which gives relevant information on the solutions.

Theorem 1 *Any optimal solution for problem* (11) *belongs to the class of functions*

$$\left\{\rho \in L^{\infty}((0, L_x) \times (0, L_y)) \ : \ \rho(x, y) \in \{-1, 1\}\right\},$$

i.e. optimal solutions just take on either -1 *or* 1.

This theorem is a simple consequence of Lemma 1 in Artstein (1980), applied to the linear functional B_k maximized on the closed convex set C of functions in $\overline{\mathcal{U}}$ verifying the linear constraints. The lemma implies that any optimal solution for (11) must be an extreme point of C (ρ is an extreme point of C if given $\rho_1, \rho_2 \in C$ and $t \in (0, 1)$ such that $\rho = t\rho_1 + (1-t)\rho_2$, then $\rho = \rho_1 = \rho_2$), and it is elementary to check that extreme points of C belong to the class of functions taking values on the set $\{-1, 1\}$.

A direct consequence of Theorem 1 is that our original optimization problem (7) admits maximizers, and very remarkable those maximizers will never take value 0 on, that is to say, we will never find with our procedure MSA such that there are regions in which we do not place electrode, we just find a polarization profile (positive or negative) of the piezoelectric MSA distributed on the whole domain.

4 Numerical approach and examples

Having discretized the rectangular sensor layer in N finite elements (typically $N \gg M$), the discrete optimization problem can be written as

$$\text{Maximize}_{\boldsymbol{\rho}} : \mathbf{F}_k^T \boldsymbol{\rho} \tag{13}$$

subject to:

$$\begin{aligned} &\mathbf{F}_j^T \boldsymbol{\rho} = 0, \text{for } j = 1, \cdots, M, \text{ and } j \neq k, \\ &-\mathbf{1} \leq \boldsymbol{\rho} \leq \mathbf{1}, \end{aligned} \tag{14}$$

where $\{\mathbf{F}_j\}_{j=1,\cdots,M}$ is the family vector of the laplacian of the first M modes (previously computed), and $\boldsymbol{\rho}$ is the vector of the design variables. This approach presents the advantage that both objective function and constraints are linear and hence, it can be easily solved by the simplex method.

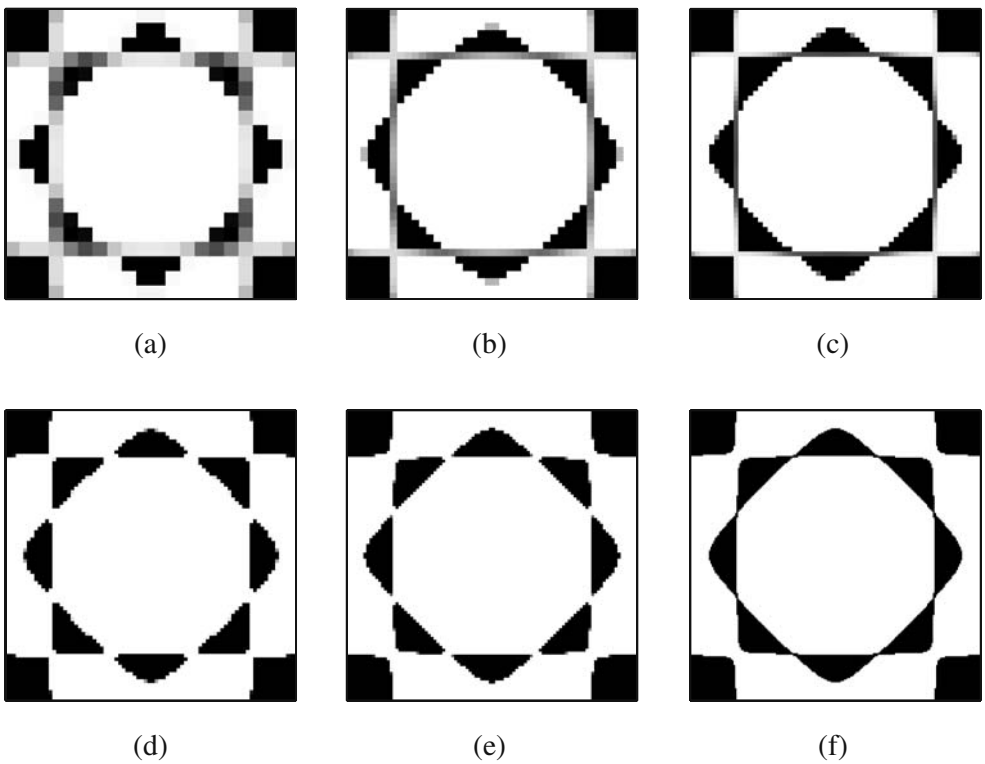

Fig. 6 Polarization profiles to isolate the first mode taking $M = 26$ for different mesh sizes. **a** 20×20. **b** 40×40. **c** 60×60. **d** 80×80. **e** 100×100. **f** 200×200

We would like to remark the value of the mathematical result of the previous section for the numerical approximation of the problem. The discretized problem consists of maximizing a linear functional subject to a number of linear constraints, and of course it makes perfect sense to look for the maximizers among the extremal points of the admissibility set, as the simplex methods does indeed. Further to this, we know that maximizers for the continuum are also extremals of the set of designs verifying the constraints, and then we

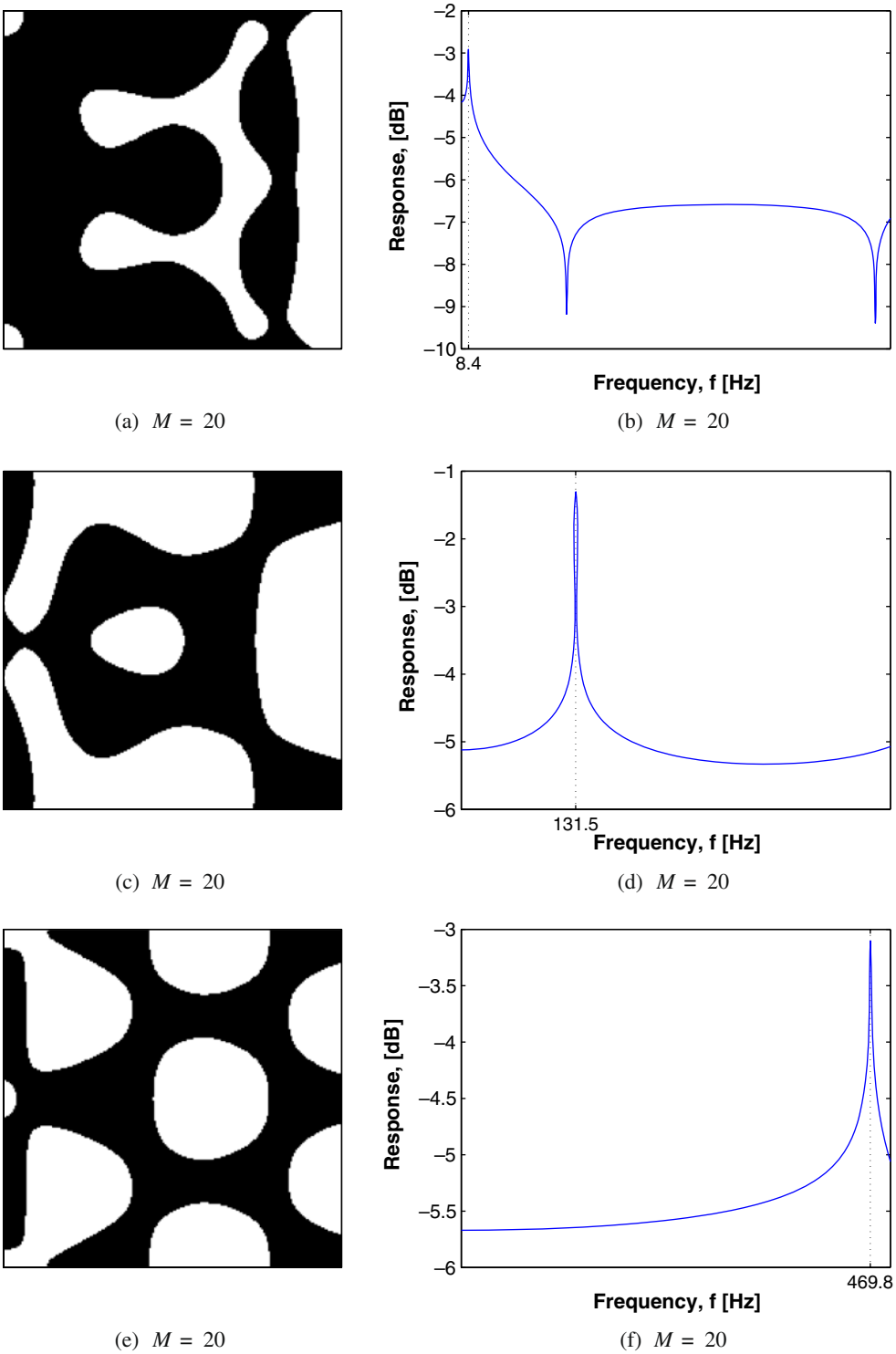

(a) $M = 20$ (b) $M = 20$

(c) $M = 20$ (d) $M = 20$

(e) $M = 20$ (f) $M = 20$

Fig. 7 Polarization profiles to isolate the first mode (**a**, **b**), the sixth mode (**c**, **d**) and the eighteenth mode (**e**, **f**) for a plate cantilevered in it left side

are actually looking for approximations of this optimal designs on using the simplex method applied to the discrete problem. This is actually corroborated by the fact that in our simulations intermediate values between -1 and 1 in the optimal profiles tend to disappear when we consider finer and finer meshes (see Fig. 6). Actually for a mesh of 200×200 elements we cannot even notice such an intermediate values in all the examples we have dealt with.

We illustrate our optimization approach through several numerical examples varying the boundary conditions in a square plate of dimensions $L_x = L_y = 1$ m and $h_p = 0.01$ m. The material properties are the corresponding to steel, that is, Young's modulus $E = 200$ GPa, Poisson's ratio $\nu = 0.3$ and mass density $\rho = 7800$ kg/m^3. In all the examples a mesh of 200×200 elements has been used to compute the mode shapes as well as to run the linear optimization problem. Both parts have been simulated by using routines already implemented in MATLAB.

4.1 Example 1: plate simply-supported at all four sides

In this first example, a four-side simply-supported plate is considered. It is well-known that, for this particular case, it is possible to find explicit formulae for both natural frequencies and mode shapes (Blevins 1985). In Fig. 3a the polarization profile corresponding to a modal sensor sensitive to the first mode and insensitive to 2–10 is shown. As we can see, at the end of the optimization process, the design variable takes on two values only: $\rho = 1$, represented by a black color, and $\rho = -1$ by a white color, meaning regions with opposite polarization (but, of course, inverting the polarization in all layer, the profile continues to be optimal because it would be the counterpart of the corresponding mode inverted in sign). The frequency response (see Fig. 3b) shows that the first mode is activated (at 47.8 Hz), the modes from 2 to 10 are filtered, but the eleventh mode is again observed (at 415.5 Hz).

However, the results perfectly agree with the constraints, because we have just limited the number of modes to ten ($M = 10$). To filter any following mode, we have just to include it by adding a new constraint in the optimization problem, but, as it was expected, the profile changes its topology as the number of modes considered increases: see for $M = 15$ (Fig. 4a and 4b), $M = 20$ (Fig. 4c and 4d), and finally $M = 26$ (Fig. 4e and 4f).

It is worthwhile emphasizing that, from a practical point of view, the layouts of Fig. 4a, 4c and 4e are as good as the one in Fig. 3a to isolate the first mode. However, from our mathematical approach as an optimization problem, on the one hand, the topology obtained for a fixed M value is better (in the sense of the cost we maximize) than the rest of topologies (obtained for a different M) for such a M value, because the latter gives similar, but slightly lower objective function value B_k, and on the other hand, it seems to be a global maximizer according to our numerical examples on using different starting guesses.

Polarization profiles that isolate the eleventh mode (at 415.5 Hz) and the eighteenth mode (at 679.4 Hz) under the same boundary conditions are also shown in Fig. 5, taking again $M = 26$.

4.2 Example 2: plate cantilevered in one side

A plate cantilevered in its left side is considered as the second example. For this case study as well as in most cases, the equation for the modes cannot be solved in closed form (for beams either) and hence, they have to be numerically obtained. Taking now $M = 20$, polarization profiles that isolate the first mode (at 8.4 Hz), the sixth mode (at 131.5 Hz) and the eleventh mode (at 469.8 Hz) for this new situation are shown in Fig. 7.

5 Conclusions

This paper has presented a new way to systematically design distributed piezoelectric MSA for plates with arbitrary boundary conditions. A linear optimization approach based on the sensor response is proposed, taking both the effective surface electrode and the polarization profile of the piezoelectric layers as the design variables. It was analytically proved, and numerically corroborated in several examples, that optimized patterns that isolate particular vibration modes correspond to entirely covering the layers by electrode ($\chi_m \equiv 1$) and polarization profiles taking on only two values. We think it would not very difficult to extend all this approach to shell structures and we plan to do it in the near future.

Acknowledgements This work has been supported by Ministerio de Educación y Ciencia MTM2007-62945 (Spain), Junta de Comunidades de Castilla-La Mancha PCI-08-0084 (Spain) and Universidad de Castilla-La Mancha TC20070059 (Spain). The authors acknowledge interesting suggestions on the subject of this paper from Martin Bendsøe and Ole Sigmund.

References

Artstein Z (1980) Discrete and continuous bang-bang and facial spaces or: look for the extreme points. SIAM Review 22(2):172–185

Bendsøe MP, Sigmund O (2003) Topology optimization—theory, methods and applications. Springer, Berlin

Blevins RD (1985) Formulas for natural frequency and mode shape. Krieger, Marburg

Clark RL, Burke SE (1996) Practical limitations in achieving shaped modal sensors with induced strain materials. J Vib Acoust 118:668–675

Clark RL, Saunders WR, Gibbs GP (1998) Adaptive structures: dynamics and control. Wiley, New York

Donoso A, Sigmund O (2008) Optimization of piezoelectric bimorph actuators with active damping for static and dynamic loads. SMO. doi:10.1007//s00158-008-0273-0

Fonseca I, Leonni G (2007) Modern methods in the calculus of variations: L^p-spaces. Springer, New York

Friswell MI (2001) On the design of modal sensors and actuators. J Sound Vib 241:361–372

Gawronski W (2000) Modal sensors and actuators. J Sound Vib 229:1013–1022

Hsu YH, Lee CK (2004) On the autononomous gain and phase tailoring transfer functions of symmetrically distributed piezoelectric sensors. J Vib Acoust 126(4):528–536.

Jian K, Friswell MI (2006) Designing distributed modal sensors for plate structures using finite element analysis. Mech Syst Signal Process 20:2290–2304

Jian K, Friswell MI (2007) Distributed modal sensors for rectangular plate structures. J Intell Mater Syst Struct 18:939–948

Kim J, Hwang JS, Kim SJ (2001) Design of modal transducers by optimizing spatial distribution of discrete gain weights. AIAA J 39:1969–1976

Kögl M, Silva ECN (2005) Topology optimization of smart structures: design of piezoelectric plate and shell actuators. Smart Mater Struct 14:387–399

Lee CK, Moon FC (1990) Modal sensors/actuators. J Appl Mech 57:434–441

Moheimani SOR, Fleming AJ (2006) Piezoelectric transducers for vibration control and damping. Springer, Heidelberg

Mukherjee A, Joshi SP (2003) A gradientless technique for optimal distribution of piezoelectric material for structural control. Int J Numer Methods Eng 57:1737–1753

Preumont A, Francois A, De Man P, Piefort V (2003) Spatial filters in structural control. J Sound Vib 265:61–79

Sun D, Tong L, Wang D (2002) Modal actuator/sensor by modulating thickness of piezoelectric layers for smart plates. AIAA J 39:1676–1679

Tartar L (2000) An introduction to the homogenization method in optimal design. Lecture note in mathematics, vol 1740. Springer, Berlin, pp 47–156